

Quantum properties of a three-level atom interacting with two radiation fields

Xiao-shen Li and Yue-nan Peng

Department of Physics, Teachers University of Jiangxi, Nanchang, Jiangxi, China

(Received 13 February 1985)

The quantum-statistical model for a three-level atom interacting with two radiation fields is studied. The mean atomic occupations and photon numbers are obtained under different initial conditions of one coherent field and one chaotic field or both chaotic or coherent fields, with the atom in upper or lower states. Through numerical summation, it is shown that the effects of coherent sources and chaotic sources are different even for low intensities. Meanwhile the effects of detuning on this interaction are discussed.

I. INTRODUCTION

In a recent paper, Li and Bei¹ extended the two-level Jaynes-Cummings model²⁻⁵ to the three-level case. In their discussions, they showed that collapses and recoveries occur explicitly even in the case of weak excitation. In this paper we study the quantum properties of a three-level atom interacting with two radiation fields, of which initially one is coherent but the other chaotic, or both chaotic or coherent. The time evolution of the expectation values of the atomic-level operators are given by using the numerical method, which shows decay and recovery. In addition the effects of equal detunings are also investigated.

II. THE MODEL

The atomic model used here is shown in Fig. 1. In the rotating-wave approximation (RWA), the Hamiltonian for this model can be expressed in terms of atomic-transition-projection operators \hat{S}_{ij} ($i, j=1, 2, 3$) and the destruction and creation operators $\hat{a}_k, \hat{a}_k^\dagger$ ($k=1, 2$) of the radiation fields as

$$\begin{aligned} \hat{H} = & \hbar\omega_a \hat{S}_{11} + \hbar \sum_{i=1}^2 \omega_{b_i} \hat{S}_{i+1, i+1} + \hbar \sum_{i=1}^2 \Omega_i \hat{a}_i^\dagger \hat{a}_i \\ & + \hbar \sum_{i=1}^2 \lambda_i (\hat{S}_{1, i+1} \hat{a}_i + \text{H.c.}), \end{aligned} \quad (1)$$

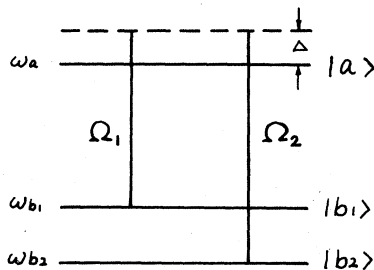


FIG. 1. Three-level atom with eigenstates $|a\rangle$, $|b_1\rangle$, and $|b_2\rangle$, eigenvalues of energy $\hbar\omega_a$, $\hbar\omega_{b_1}$, and $\hbar\omega_{b_2}$, respectively. The atomic transition between $|a\rangle$ and $|b_1\rangle$ ($|b_2\rangle$) is mediated by mode 1 (2) with frequency Ω_1 (Ω_2).

where $\hbar\omega_\alpha$ ($\alpha=a, b_1, b_2$) is the energy of atomic level $|\alpha\rangle$ and λ_i and Ω_i are the coupling constant and frequency for mode i , respectively.

The atomic states are

$$|a\rangle = \begin{bmatrix} 1 \\ 0 \\ 0 \end{bmatrix}, \quad |b_1\rangle = \begin{bmatrix} 0 \\ 1 \\ 0 \end{bmatrix}, \quad |b_2\rangle = \begin{bmatrix} 0 \\ 0 \\ 1 \end{bmatrix}. \quad (2a)$$

The \hat{S} 's are 3×3 matrices, of which the elements can be expressed as

$$(\hat{S}_{ij})_{kl} = \delta_{ki} \delta_{jl}. \quad (2b)$$

They are the generators of the unitary U(3) group and obey the following relations:

$$[\hat{S}_{ij}, \hat{S}_{kl}] = \hat{S}_{il} \delta_{jk} - \hat{S}_{kj} \delta_{li}, \quad (3)$$

$$[\hat{S}_{kl}, \hat{a}_n] = [\hat{S}_{kl}, \hat{a}_n^\dagger] = 0, \quad n=1, 2. \quad (4)$$

The Hamiltonian can be rewritten as

$$\hat{H} = \hbar(\hat{H}_0 + \hat{V}), \quad (5)$$

where the "free part"

$$\begin{aligned} \hat{H}_0 = & \omega_a \hat{S}_{11} + \sum_{i=1}^2 (\omega_{b_i} \hat{S}_{i+1, i+1} + \Omega_i \hat{a}_i^\dagger \hat{a}_i) \\ & + \frac{\Delta}{2} (\hat{S}_{11} - \hat{S}_{22} - \hat{S}_{33}), \end{aligned} \quad (6)$$

and the "interaction part"

$$\hat{V} = \sum_{i=1}^2 \lambda_i (\hat{S}_{1, i+1} \hat{a}_i + \text{H.c.}) - \frac{1}{2} \Delta (\hat{S}_{11} - \hat{S}_{22} - \hat{S}_{33}), \quad (7)$$

where

$$\Delta = \Omega_i - (\omega_a - \omega_{b_i}) \quad (8)$$

is the equal detuning.

By using Eqs. (3) and (4), \hat{H}_0 and \hat{V} can be shown to be motion constants, i.e.,

$$[\hat{H}_0, \hat{H}] = [\hat{V}, \hat{H}] = [\hat{H}_0, \hat{V}] = 0. \quad (9)$$

So in the "interaction picture" the time evolution operator $\hat{U}(t, 0)$ can be written as

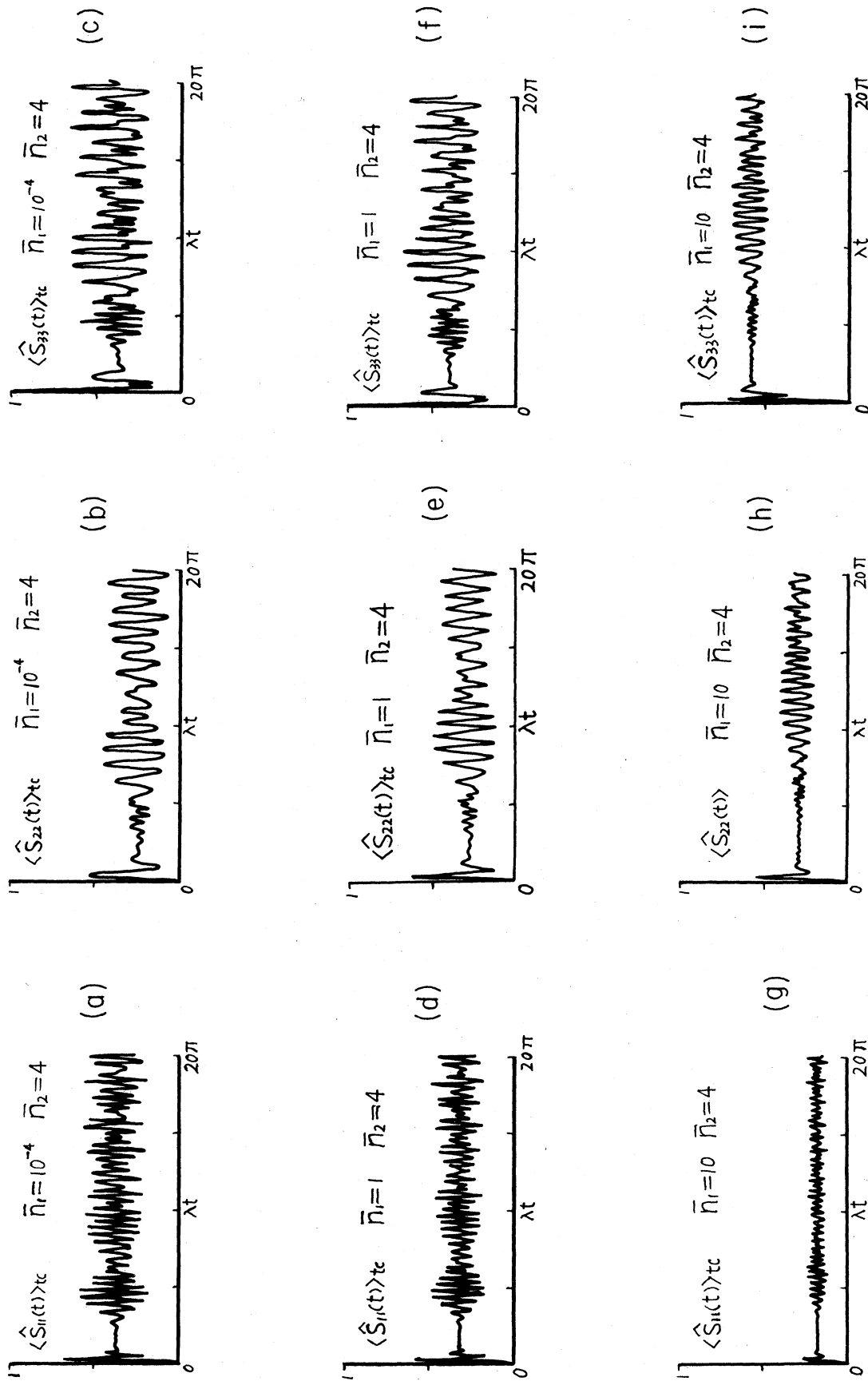


FIG. 2. (a)–(i) show short times from computer summation of Eqs. (18)–(20), $\Delta = 0$, $\lambda_1 = \lambda_2 = \lambda$.

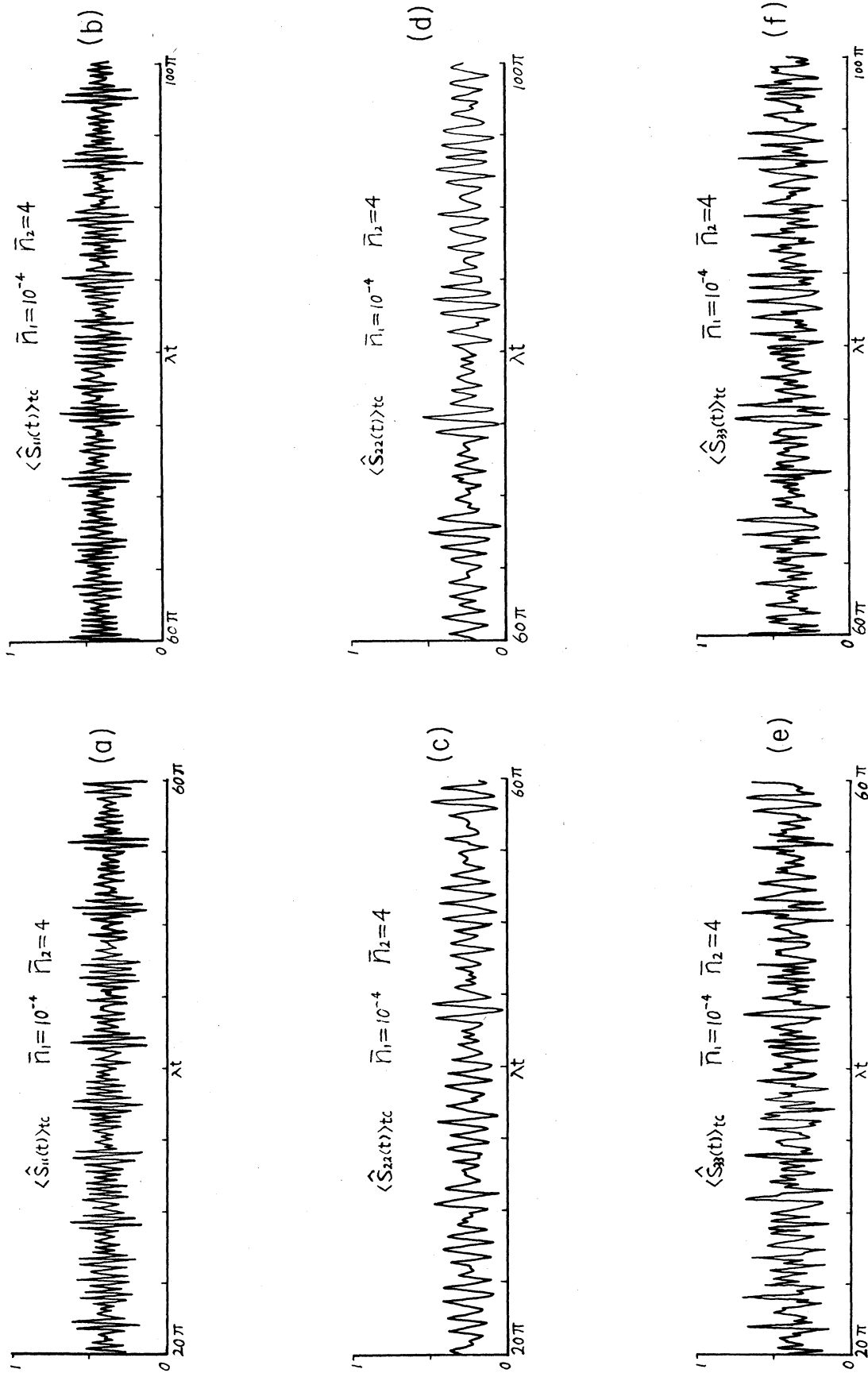


FIG. 3. (a)–(f) show long times from computer summation of Eqs. (18)–(20), $\Delta = 0$, $\lambda_1 = \lambda_2 = \lambda$.

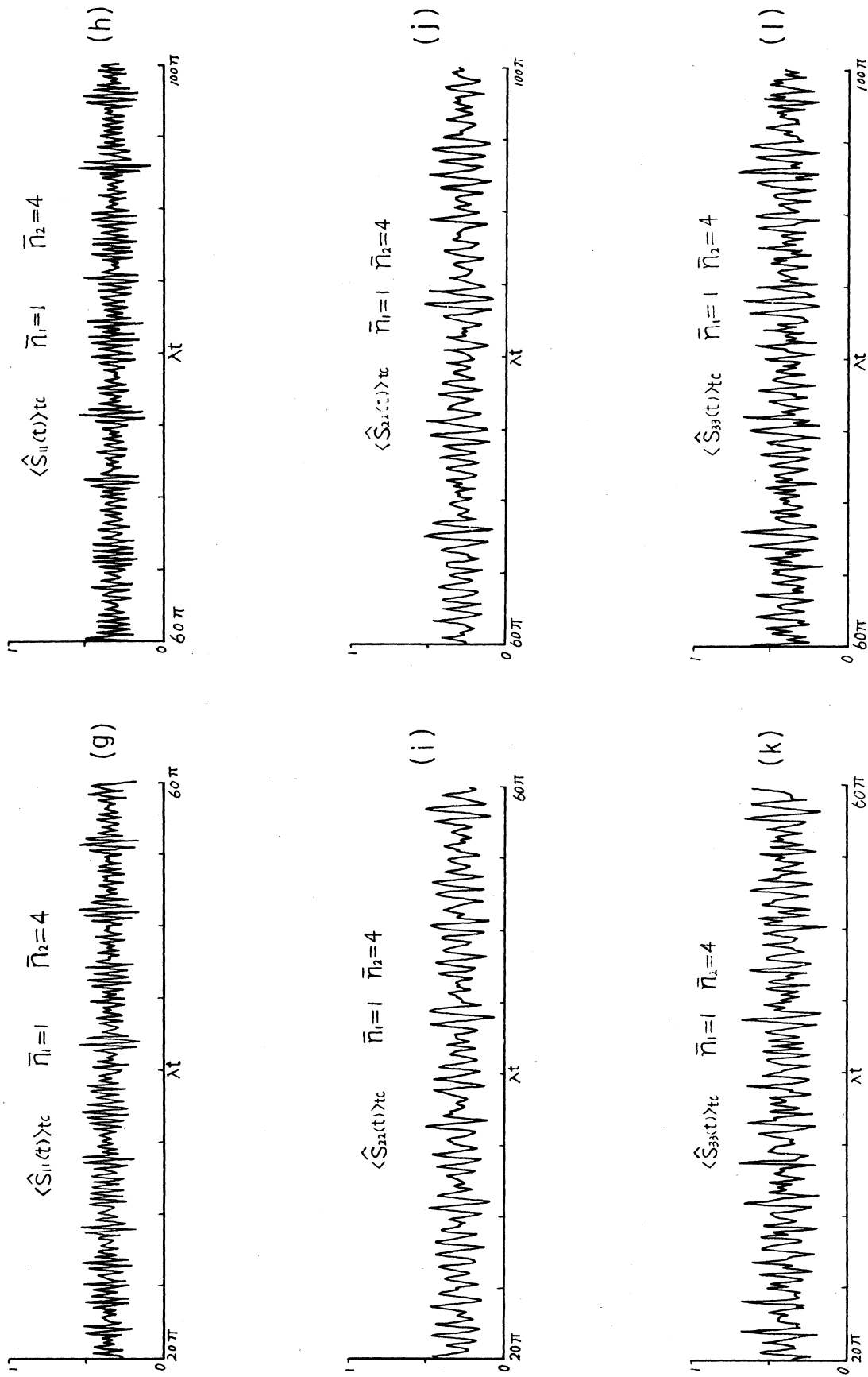


FIG. 3. (Continued).

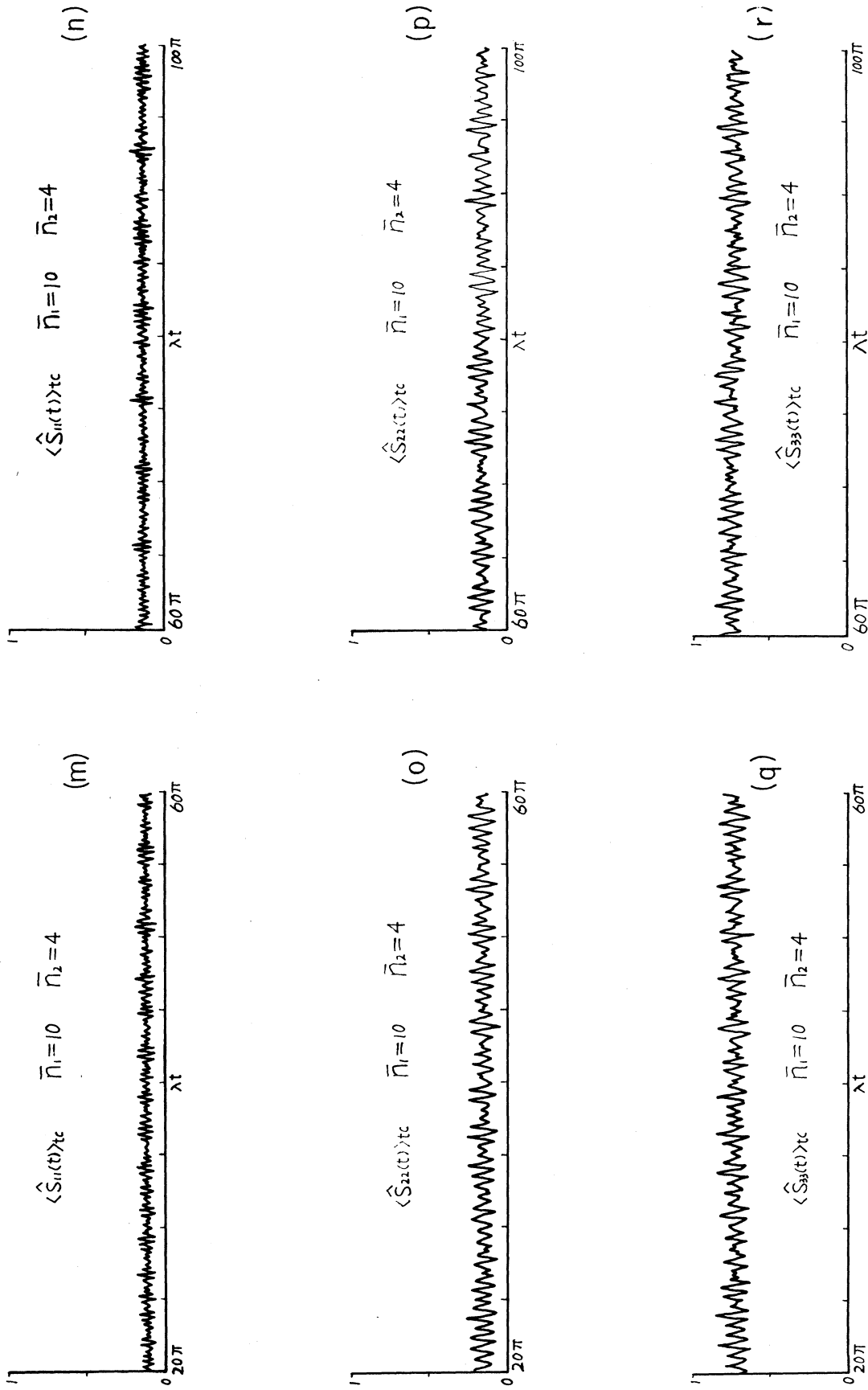


FIG. 3. (Continued).

$$\langle \hat{S}_{11}(t) \rangle_{tc} = \lambda_2^2 \sum_{n_1, n_2} n_2 \sin^2(\sqrt{\mu_2}t) P_{tc}(n_1, n_2 | \bar{n}_1, \bar{n}_2) / \mu_2, \quad (18)$$

$$\begin{aligned} \langle \hat{S}_{22}(t) \rangle_{tc} = & \lambda_1^2 \lambda_2^2 \sum_{n_1, n_2} (n_1 + 1) n_2 [\cos^2(\sqrt{\mu_2}t) + \Delta^2 \sin^2(\sqrt{\mu_2}t) / 4\mu_2 - 2 \cos(\Delta t / 2) \cos(\sqrt{\mu_2}t) \\ & - \Delta \sin(\Delta t / 2) \sin(\sqrt{\mu_2}t) / \sqrt{\mu_2 + 1}] P_{tc}(n_1, n_2 | \bar{n}_1, \bar{n}_2) / \beta_2^2, \end{aligned} \quad (19)$$

$$\langle \hat{S}_{33}(t) \rangle \equiv 1 - \langle \hat{S}_{11}(t) \rangle - \langle \hat{S}_{22}(t) \rangle, \quad (20)$$

where

$$P_{tc}(n_1, n_2 | \bar{n}_1, \bar{n}_2) = \bar{n}_1^{n_1} \bar{n}_2^{n_2} \exp(-\bar{n}_2) / (\bar{n}_1 + 1)^{n_1 + 1} n_2!, \quad (21)$$

$$\beta_2 = \lambda_1^2 (n_1 + 1) + \lambda_2^2 n_2, \quad (22)$$

$$\mu_2 = \beta_2 + \Delta^2 / 4. \quad (23)$$

The subscripts t and c express chaotic field and coherent field, respectively. The following may be inferred by analogy.

In the same way, the mean photon numbers are found to be

$$\langle \hat{n}_1(t) \rangle_{tc} = \bar{n}_1 + \langle \hat{S}_{22}(t) \rangle_{tc}, \quad (24)$$

$$\langle \hat{n}_2(t) \rangle_{tc} = \bar{n}_2 - \langle \hat{S}_{11}(t) \rangle_{tc} - \langle \hat{S}_{22}(t) \rangle_{tc}. \quad (25)$$

From Eqs. (24) and (25) we can see that when $t > 0$, mode 2 will be weakened via stimulated absorption ($|b_2\rangle \rightarrow |a\rangle$) and the two-photon transition ($|b_2\rangle \rightarrow |b_1\rangle$) accompanied by absorbing a photon of

mode 2 and emitting a photon of mode 1, but mode 1 will be amplified in the same process. By means of numerical summation, we can see the evolution of the average atomic occupations (see Figs. 2 and 3). Figure 2 shows that there exists only one recovery, i.e., the first one. It seems that the coherent field (mode 2) is not strong enough to separate the tail of the beginning of the second recovery and that stronger chaotic field (mode 1) will result in a longer recovery time, shorter collapse time, and smaller oscillation amplitude. The latter phenomenon can also be seen from Fig. 3, which makes it clear that stronger chaotic-field mode 1 will cancel the effects of the coherent mode 2. Similar to Ref. 1, an increase of \bar{n}_1 will cause the $\langle \hat{S}_{11}(t) \rangle_{tc}$ curve to shift downwards and the $\langle \hat{S}_{33}(t) \rangle_{tc}$ to shift upwards but evidently will not cause the $\langle \hat{S}_{22}(t) \rangle_{tc}$ curve to shift. In addition long-time behavior (as long as $100\lambda\pi$) of the oscillations shows no evident damping.

IV. INITIALLY TWO CHAOTIC FIELDS

Here we consider that the atom starts in $|b_2\rangle$ and the two modes initially in chaotic states, i.e.,

$$\hat{\rho}_F(0) = \sum_{m_1, m_2} \frac{\bar{n}_1^{m_1}}{(\bar{n}_1 + 1)^{m_1 + 1}} \frac{\bar{n}_2^{m_2}}{(\bar{n}_2 + 1)^{m_2 + 1}} |m_1, m_2\rangle \langle m_1, m_2|. \quad (26)$$

So it is found that

$$\langle \hat{S}_{11}(t) \rangle_u = \lambda_2^2 \sum_{n_1, n_2} n_2 \sin^2(\sqrt{\mu_2}t) P_u(n_1, n_2 | \bar{n}_1, \bar{n}_2) / \mu_2, \quad (27)$$

$$\begin{aligned} \langle \hat{S}_{22}(t) \rangle_u = & \lambda_1^2 \lambda_2^2 \sum_{n_1, n_2} (n_1 + 1) n_2 [\cos^2(\sqrt{\mu_2}t) + \Delta^2 \sin^2(\sqrt{\mu_2}t) / 4\mu_2 - 2 \cos(\Delta t / 2) \cos(\sqrt{\mu_2}t) \\ & - \Delta \sin(\Delta t / 2) \sin(\sqrt{\mu_2}t) / \sqrt{\mu_2 + 1}] P_u(n_1, n_2 | \bar{n}_1, \bar{n}_2) / \beta_2^2, \end{aligned} \quad (28)$$

where

$$P_u(n_1, n_2 | \bar{n}_1, \bar{n}_2) = \bar{n}_1^{n_1} \bar{n}_2^{n_2} / (\bar{n}_1 + 1)^{n_1 + 1} (\bar{n}_2 + 1)^{n_2 + 1}. \quad (29)$$

In this case, Eqs. (20), (24), and (25) are also valid.

Numerically calculated from Eqs. (27), (28), and (20), Figs. 4 and 5 show the behavior of the average atomic occupations. From Figs. 4(d) and 4(g)—4(i), we see that there exists collapse and recovery in the case of two initial chaotic fields as well as two initial coherent fields.¹ This means that no matter if the two initial fields are coherent or chaotic, partial recurrences of the collapsed initial state⁵ will occur. Figure 4(a)—4(c) show that \bar{n}_1 is not large enough to separate the tail of the beginning of the first recovery. Evidently, the larger \bar{n}_1 or \bar{n}_2 , the smaller the amplitudes of the oscillations and the longer the recovery time will be. Because of the above effects we may expect that it is difficult for the second recovery to occur apparently, even if we have larger \bar{n}_1 or \bar{n}_2 . In addition Fig. 5 shows no trend of decay.

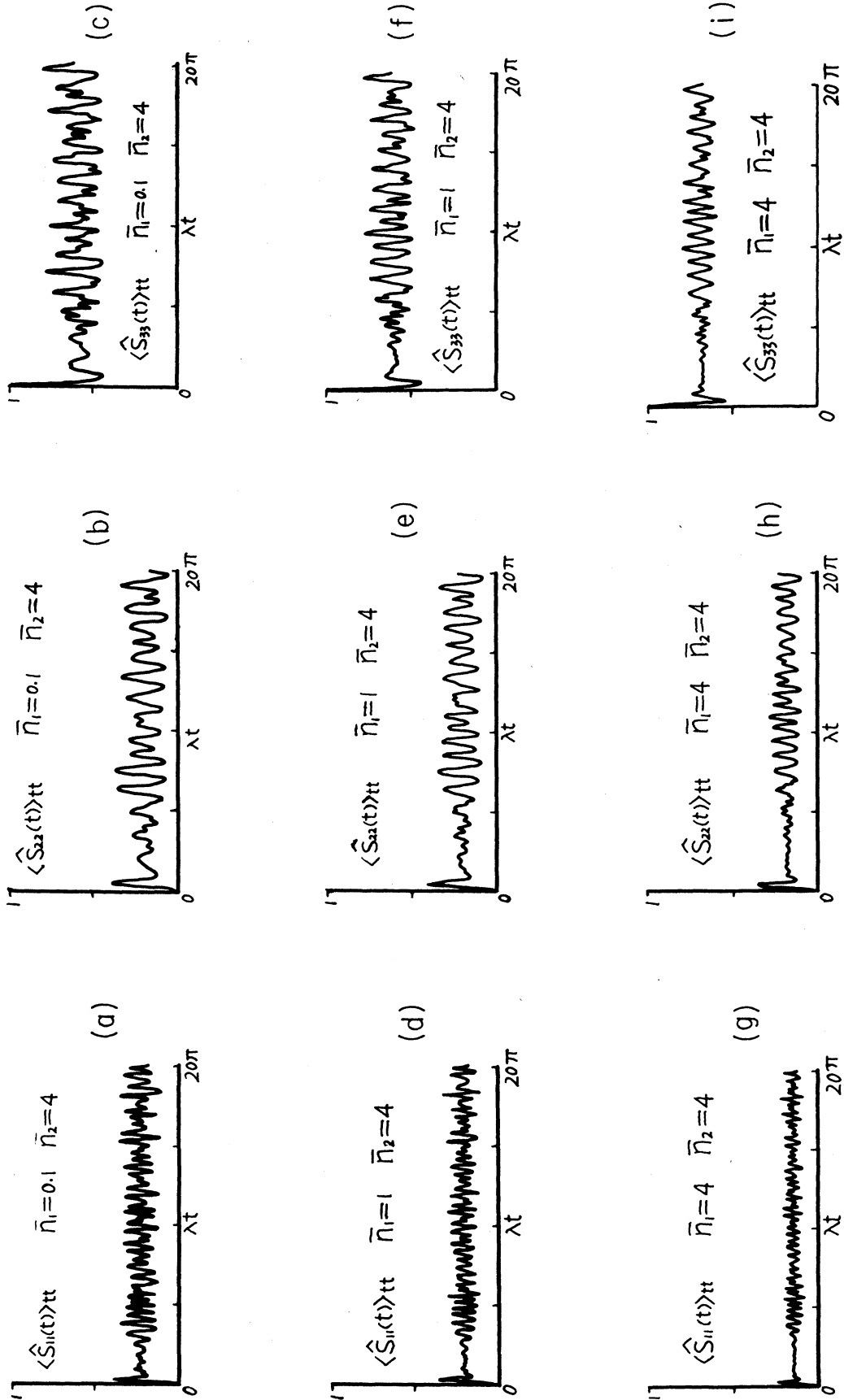


FIG. 4. (a)–(i) show short times from computer summation of Eqs. (27), (28), and (20), $\Delta=0, \lambda_1=\lambda_2=\lambda$.

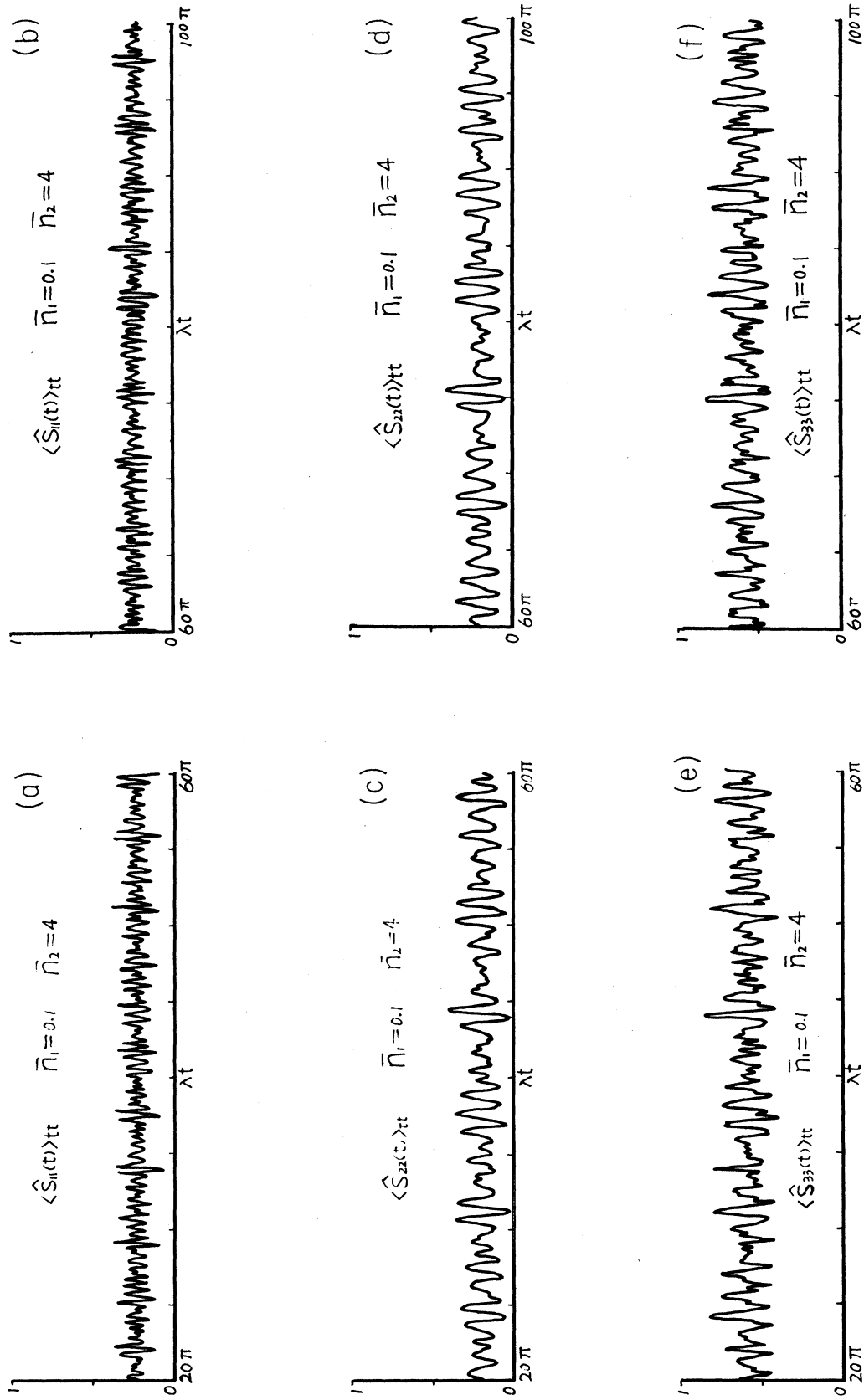


FIG. 5. (a)–(f) show long times from computer summation of Eqs. (27), (28), and (20), $\Delta = 0$, $\lambda_1 = \lambda_2 = \lambda$.

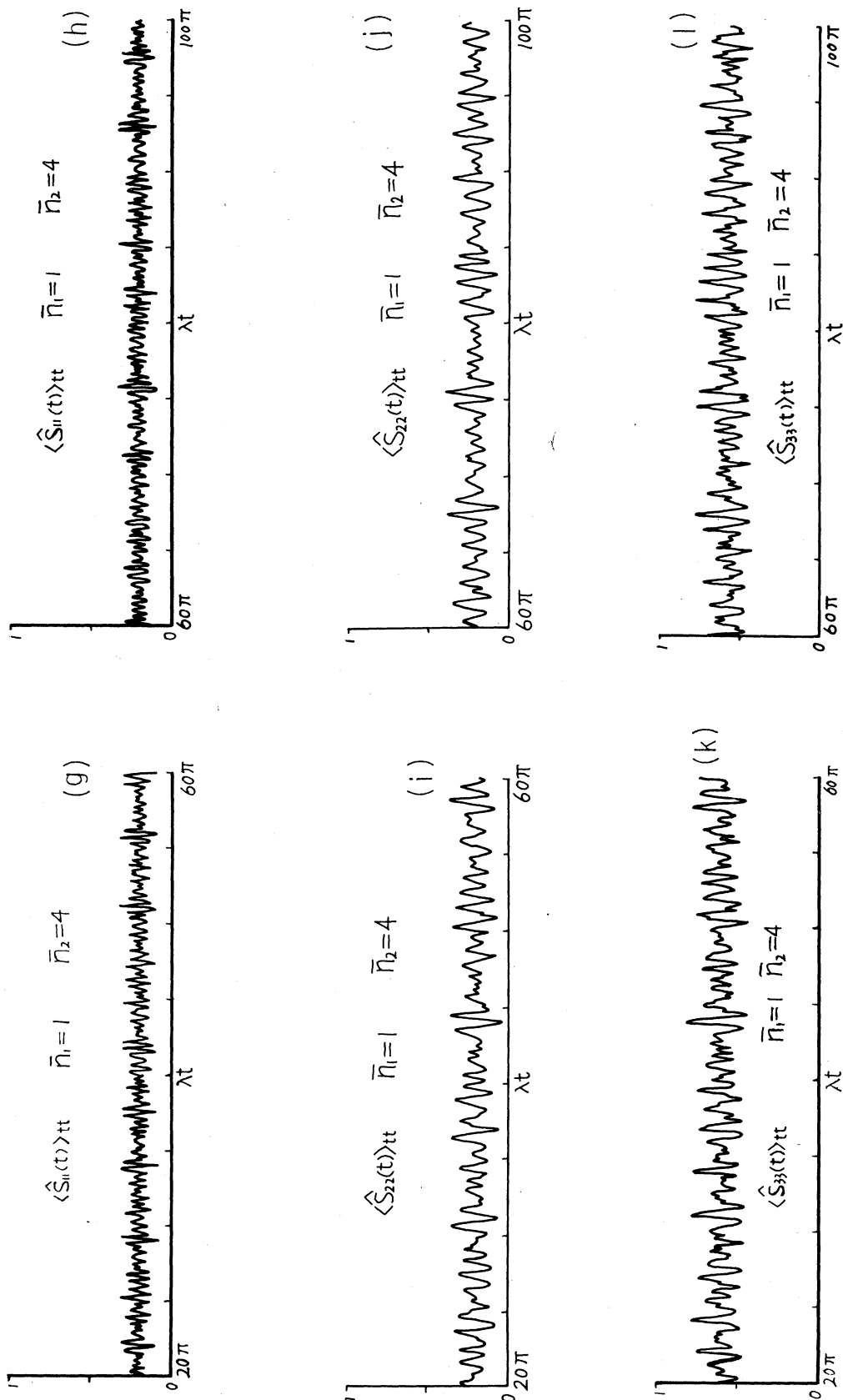


FIG. 5. (Continued).

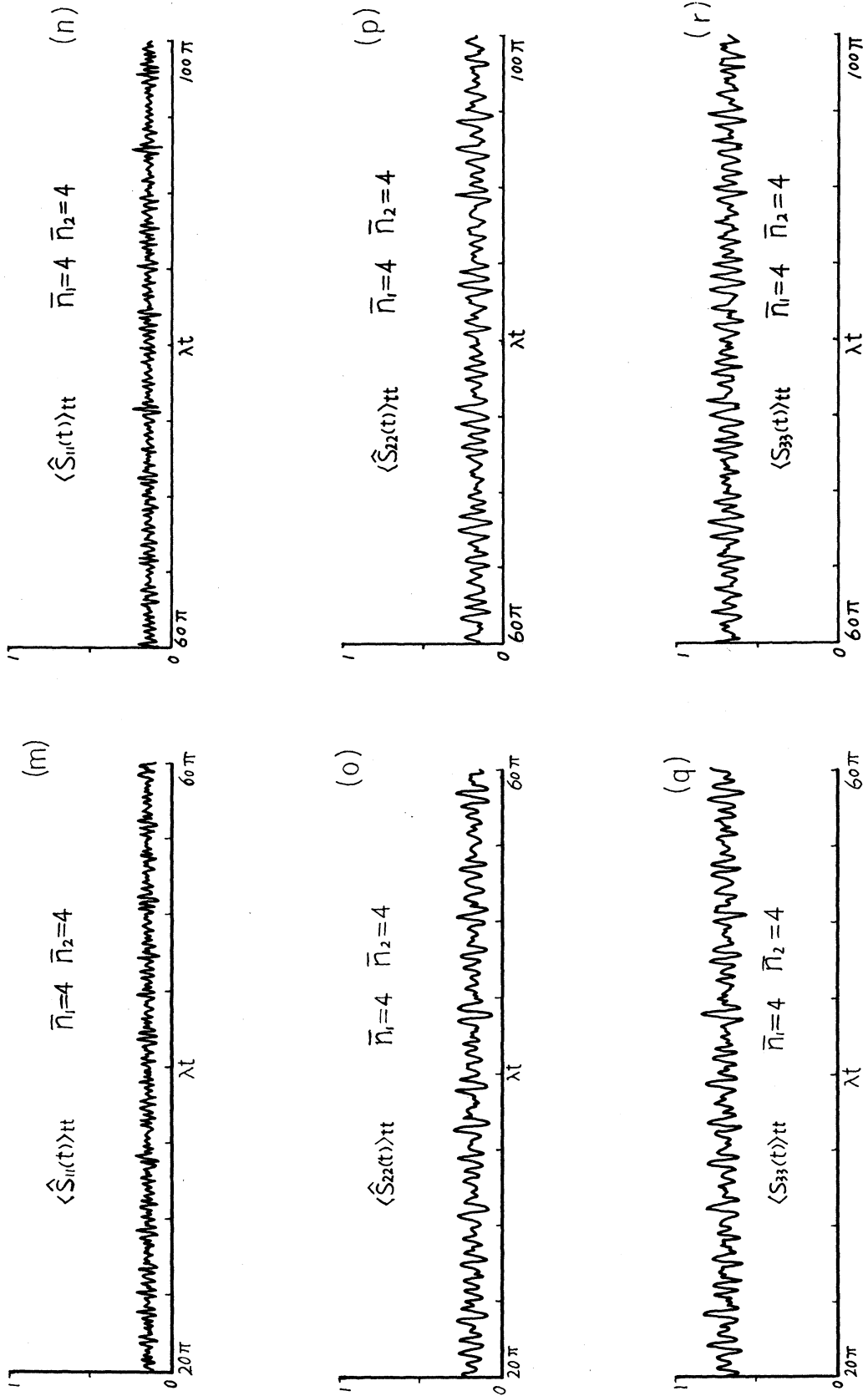


FIG. 5. (Continued).

V. THE EFFECTS OF THE DETUNING

A. Initially two coherent fields

When the two modes are initially in the coherent states $|\alpha_1\rangle$ and $|\alpha_2\rangle$, respectively, the density operator will be

$$\hat{\rho}_F(0) = \sum_{m_1, m'_1, m_2, m'_2} \exp(-\bar{n}_1 - \bar{n}_2) \frac{\alpha_1^{m_1} (\alpha_1^*)^{m'_1} \alpha_2^{m_2} \alpha_2^{m'_2}}{(m_1! m'_1! m_2! m'_2!)^{1/2}} |m_1, m_2\rangle \langle m'_1, m'_2|. \quad (30)$$

1. The atom starts in $|b_2\rangle$

In this case, the mean atomic occupations are found to be

$$\langle \hat{S}_{11}(t) \rangle_{cc} = \lambda_2^2 \sum_{n_1, n_2} n_2 \sin^2(\sqrt{\mu_2} t) P_{cc}(n_1, n_2 | \bar{n}_1, \bar{n}_2) / \mu_2, \quad (31)$$

$$\begin{aligned} \langle \hat{S}_{22}(t) \rangle_{cc} = & \lambda_1^2 \lambda_2^2 \sum_{n_1, n_2} (n_1 + 1) n_2 [\cos^2(\sqrt{\mu_2} t) + \Delta^2 \sin^2(\sqrt{\mu_2} t) / 4\mu_2 - 2 \cos(\Delta t / 2) \cos(\sqrt{\mu_2} t) \\ & - \Delta \sin(\Delta t / 2) \sin(\sqrt{\mu_2} t) / \sqrt{\mu_2 + 1}] P_{cc}(n_1, n_2 | \bar{n}_1, \bar{n}_2) / \beta_2^2, \end{aligned} \quad (32)$$

where

$$P_{cc}(n_1, n_2 | \bar{n}_1, \bar{n}_2) = \bar{n}_1^{n_1} \bar{n}_2^{n_2} \exp(-\bar{n}_1 - \bar{n}_2) / n_1! n_2!. \quad (33)$$

Figures 6(a)–6(c) show the numerical results calculated from Eqs. (31), (32), and (20). Evidently large detuning will suppress the oscillation of $\langle \hat{S}_{11}(t) \rangle_{cc}$ and lower the oscillating frequencies of $\langle \hat{S}_{22}(t) \rangle_{cc}$ and $\langle \hat{S}_{33}(t) \rangle_{cc}$. Meanwhile, the phases of $\langle \hat{S}_{22}(t) \rangle_{cc}$ and $\langle \hat{S}_{33}(t) \rangle_{cc}$ are just the opposite, i.e., there exist two-photon processes.¹ Large detuning will enhance this two-photon effect. The above phenomenon means that as detuning becomes larger, the probability of the atom staying in the upper state $|a\rangle$ will approach to zero (i.e., single-photon processes tend to disappear) and there exist only two-photon processes.

2. The atom starts in $|a\rangle$

In this case

$$\hat{\rho}(0) = \begin{pmatrix} \hat{\rho}_F(0) & 0 & 0 \\ 0 & 0 & 0 \\ 0 & 0 & 0 \end{pmatrix}, \quad (16')$$

the mean atomic occupations are found to be

$$\begin{aligned} \langle \hat{S}_{11}(t) \rangle_{cc}^a = & \sum_{n_1, n_2} [\cos^2(\sqrt{\mu} t) + \Delta^2 \sin^2(\sqrt{\mu} t) / 4\mu] \\ & \times P_{cc}(n_1, n_2 | \bar{n}_1, \bar{n}_2), \end{aligned} \quad (34)$$

$$\begin{aligned} \langle \hat{S}_{22}(t) \rangle_{cc}^a = & \lambda_1^2 \sum_{n_1, n_2} (n_1 + 1) \sin^2(\sqrt{\mu} t) \\ & \times P_{cc}(n_1, n_2 | \bar{n}_1, \bar{n}_2) / \mu, \end{aligned} \quad (35)$$

where

$$\mu = \lambda_1^2 (n_1 + 1) + \lambda_2^2 (n_2 + 1) + \Delta^2 / 4. \quad (36)$$

In the same way, the mean photon numbers in this case are found to be

$$\langle \hat{n}_1(t) \rangle^a = \bar{n}_1 + \langle \hat{S}_{22}(t) \rangle_{cc}^a, \quad (24')$$

$$\langle \hat{n}_2(t) \rangle^a = \bar{n}_2 + \langle \hat{S}_{33}(t) \rangle_{cc}^a. \quad (25')$$

From Eqs. (24') and (25') we can see that both the two modes are amplified by stimulated emission of the atom.

Numerically calculated from Eqs. (34), (35), and (20), the behavior of the mean atomic occupations are shown in Figs. 7(a)–7(c). Figure 7 shows that increasing detuning will cause the oscillations of $\langle \hat{S}_{22}(t) \rangle_{cc}^a$ and $\langle \hat{S}_{33}(t) \rangle_{cc}^a$ as

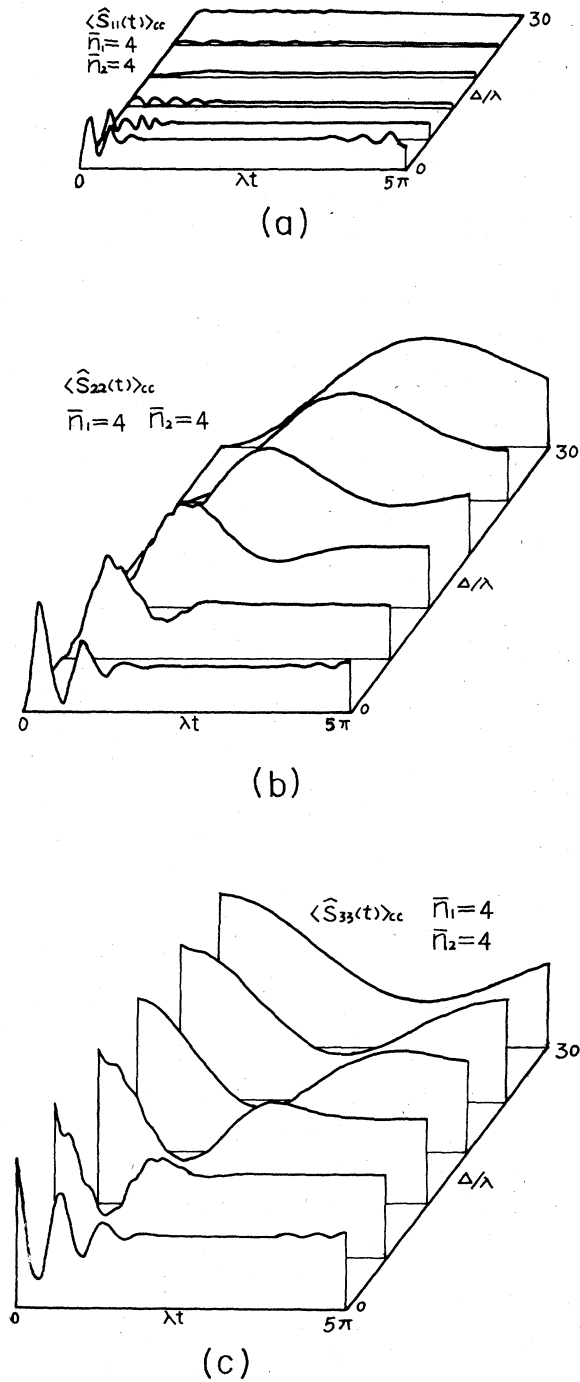


FIG. 6. (a)–(c) show curves for six spaced values of Δ/λ from computer summation of Eqs. (31), (32), and (20), $\lambda_1 = \lambda_2 = \lambda$.

well as $\langle \hat{S}_{11}(t) \rangle_{cc}^a$ to be suppressed. Furthermore, the atom will stay in the initial state $|a\rangle$ forever when there is large detuning, such as $\Delta = 30\lambda$.

In addition, from Figs. 7(b) and 7(c) we can see that the oscillation phases of $\langle \hat{S}_{22}(t) \rangle_{cc}^a$ and $\langle \hat{S}_{33}(t) \rangle_{cc}^a$ are the

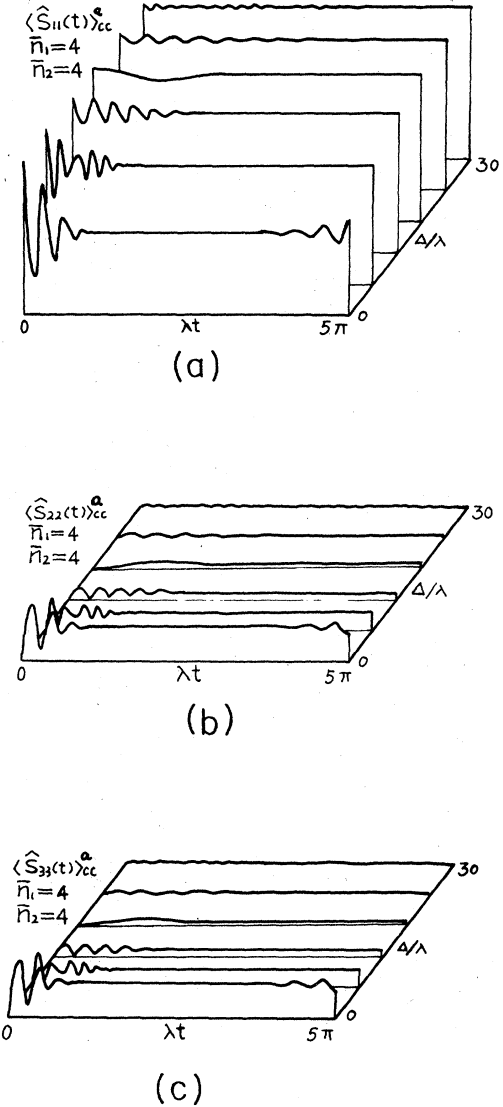


FIG. 7. (a)–(c) show curves for six spaced values of Δ/λ from computer summation of Eqs. (34), (35), and (20), $\lambda_1 = \lambda_2 = \lambda$.

same, i.e., there exist no two-photon processes but single-photon processes.

B. Initially two chaotic fields

When the atom starts in $|b_2\rangle$, the expressions for $\langle \hat{S}_{ii}(t) \rangle_u$ ($i=1,2,3$) have already been given by Eqs. (27), (28), and (20), according to which Figs. 8(a)–8(c) show the time behaviors. When the atom starts in $|a\rangle$, we can find that

$$\langle \hat{S}_{11}(t) \rangle_u^a = \sum_{n_1, n_2} [\cos^2(\sqrt{\mu}t) + \Delta^2 \sin^2(\sqrt{\mu}t)/4\mu] \times P_u(n_1, n_2 | \bar{n}_1, \bar{n}_2), \quad (37)$$

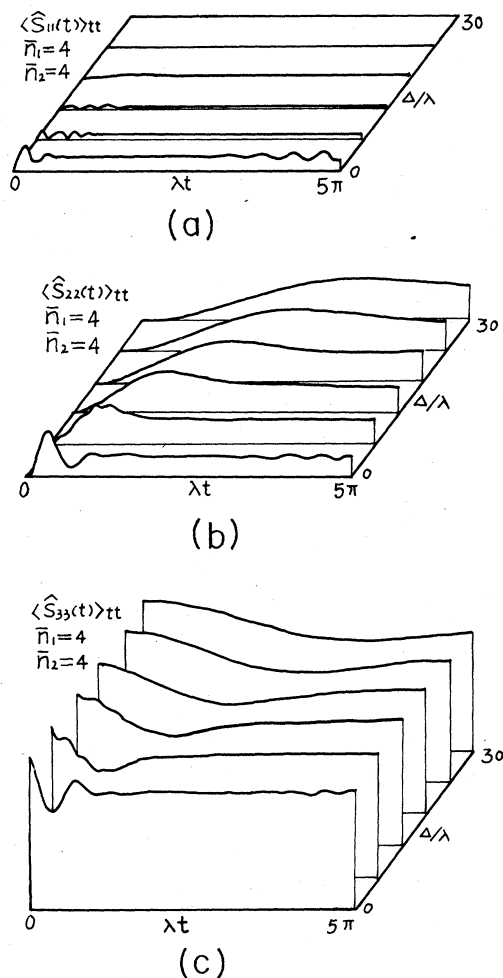


FIG. 8. (a)–(c) show curves for six spaced values of Δ/λ from computer summation of Eqs. (27), (28), and (20), $\lambda_1 = \lambda_2 = \lambda$.

$$\langle \hat{S}_{22}(t) \rangle_{tt}^a = \lambda_1^2 \sum_{n_1, n_2} (n_1 + 1) \sin^2(\sqrt{\mu t}) P_u(n_1, n_2 | \bar{n}_1, \bar{n}_2) / \mu. \quad (38)$$

Through numerical summation, Fig. 9 shows the time evolution of $\langle \hat{S}_{ii}(t) \rangle_{tt}^a$.

It is clear that $\langle \hat{S}_{ii}(t) \rangle_{tt}^a$ [$\langle \hat{S}_{ii}(t) \rangle_{tt}$], have similar behaviors to $\langle \hat{S}_{ii}(t) \rangle_{cc}^a$ [$\langle \hat{S}_{ii}(t) \rangle_{cc}$], except that the oscillation amplitudes of $\langle \hat{S}_{ii}(t) \rangle_{tt}^a$ and $\langle \hat{S}_{ii}(t) \rangle_{tt}$ are smaller. This implies that for the same intensities, the effects of the coherent fields are stronger than those of the chaotic fields.

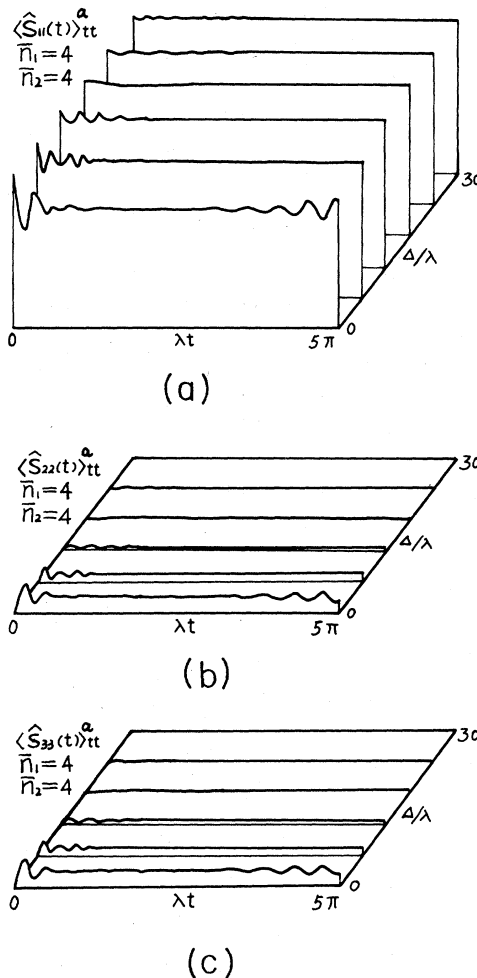


FIG. 9. (a)–(c) show curves for six spaced values of Δ/λ from computer summation of Eqs. (37), (38), and (20), $\lambda_1 = \lambda_2 = \lambda$.

VI. SUMMARY

In this paper we have exhibited new features of the three-level Jaynes-Cummings model. We have shown that recoveries (i.e., partial recurrences of the collapsed initial state) occur in the case of two initially chaotic fields as well as coherent fields. There is obvious difference in the effects of coherent sources and chaotic sources even for low intensity. In addition, large detuning will affect two-photon processes as well as single-photon stimulated emission.

¹X. S. Li and N. Y. Bei, Phys. Lett. A **101**, 169 (1984).

²E. T. Jaynes and F. W. Cummings, Proc. IEEE **51**, 89 (1963).

³J. H. Eberly, N. B. Narozhny, and J. J. Sanchez-Mondragon, Phys. Rev. Lett. **44**, 1323 (1980).

⁴S. Singh, Phys. Rev. A **25**, 3206 (1982).

⁵N. B. Narozhny, J. J. Sanchez-Mondragon, and J. H. Eberly, Phys. Rev. A **23**, 236 (1981).